NoF. R. Note No. 419/1960
Research Programme Objective E1/9

DEPARTMENT OF SCIENTIFIC AND INDUSTRIAL RESEARCH AND FIRE OFFICES' COMMITTEE
JOINT FIRE RESEARCH ORGANIZATION

ROOF VENTING OF BURNING ENCLOSURES

PART III. VENTING FIRES OF CONSTANT HEAT OUTPUT

by

P. H. Thomas, D. L. Simms, P. L. Hinkley and C. R. Theobald

This work has been done in conjunction with Messrs. COLT VENTILATION LTD.

Summary

Investigations using a 1/12 scale model representing one bay of a factory have shown that, where the area of the fire is small and its heat output is known, use can be made of Bernoulli's theorem and the theory of turbulent plumes to calculate the rates of discharge of heat and air through a vent and beneath a curtain extending from the ceiling, the temperatures near the ceiling and the depth of the layer of hot air. Formulae are given for the effect on these quantities of varying the size of the vent and the depth of the curtain. Some of the effects of the shape and position of the vents are also discussed.

February 1960

F.1000/12/346

Fire Research Station,
Boreham Wood,
HERTS.

Notation and units used in this series

Symbol	Meaning	Dimensions		Conversion factor used F.P.S. units to C.G.S. units
		F.P.S. units	C.G.S. units	
A_f	Effective area of fire	ft^2	cm^2	929
A_i	Area of inlet	ft^2	cm^2	929
A_v	Area of vent	ft^2	cm^2	929
C_d	Coefficient of discharge through the vent	-	-	-
C'_d	Coefficient of discharge beneath the curtain	-	-	-
C_p	Specific heat at constant pressure	B.T.U lb^{-1} $^oF^{-1}$	cal gm^{-1} $^oC^{-1}$	1
d	Depth of layer of hot air	ft	cm	30.5
d_c	Depth of layer of hot air beneath curtain	ft	cm	30.5
g	Acceleration due to gravity	ft/s^2	cm/s^2	30.5
h	Height of opening	ft	cm	30.5
H	Height of model	ft	cm	30.5
H_c	Depth of curtain	ft	cm	30.5
H'	$H + 1.5\sqrt{A_f}$ (effective height of model)	ft	cm	30.5
K	Thermal conductivity	B.T.U.s^{-1} ft^{-1} $^oF^{-1}$	cal s^{-1} cm^{-1} $^oC^{-1}$	15
L	Characteristic height dimension	ft	cm	30.5
l	Path length of air in model	ft	cm	30.5
M	Mass flow rate	lb/s	gm/s	454
Q	Rate of flow of heat	B.T.U/s	cal/s	252
Q_f	Heat output of fire	B.T.U/s	cal/s	252
T	Absolute temperature	^oR	^oK	0.555
T_o	" ambient "	^oR	^oK	0.555
t	Time	s	s	-
V	Volume flow rate	ft^3/s	cm^3/s	2.84×10^4
v	Velocity of gas at any given point in prototype and model)	ft/s	cm/s	30.5
w	Width of inlet	ft	cm	30.5
y	Distance measured vertically from floor	ft	cm	30.5
θ	Temperature above ambient at any given point in prototype and model	^oF	^oC	0.555
ρ	Density	lb/ft^3	gm/cm^3	0.0160

Subscripts

H = Near the ceiling
c = Level with the bottom of the curtain
o = Ambient condition
s = Discharge under the edge of the curtain
v = Discharge through the vent
y = At a distance, y, above the floor
b = At the base of the hot layer
i = Inlet

ROOF VENTING OF BURNING ENCLOSURES

PART III. VENTING FIRES OF CONSTANT HEAT OUTPUT

by

P. H. Thomas, D. L. Simms, P. L. Hinkley and C. R. Theobald

1. Introduction

A previous note[1] described the construction of a 1/12 scale model of a bay of a factory for use in studying the effect of venting burning enclosures. The present paper describes the experiments that have been made with this model to examine the influence of the size, shape and position of the vent, the depth of any auxiliary curtains and the shape and area of the heat source on the temperature distribution in the model and the heat flow through it. The results are shown to agree with calculations based on a simplified theoretical approach to the venting of fires derived from Bernoulli's theorem and the theory of turbulent plumes[2].

The application of the theory to larger and differently shaped enclosures, larger fires and the design of venting systems will be discussed in later papers.

2. Experimental method and results

2.1. Apparatus and procedure

The model is shown in fig. 1. Essentially it is an asbestos box insulated on the outside with exfoliated vermiculite and lined on the inside with aluminium foil. Heat was supplied by various types of gas burner (fig. 2) the gas input being regulated to give a gross heat output of 2.37 B.T.U/s. The earlier experiments[3], showed that there were two time constants governing the equilibrium temperature rise; a short one associated with the air flow and a long one of less importance associated with the walls. In each experiment the walls were allowed to reach equilibrium. Measurements were then made of the air temperatures at various points inside the model and of the distribution of air velocity and temperature along the vertical centre line of the inlet. The temperatures were measured using 44 S.W.G. chromel-alumel thermocouples distributed as shown in fig. 1A except for a few of the early experiments where they were shown in fig. 1B. Air velocities were measured with a radiation compensated Simmonds anemometer[4]. Since the horizontal distributions of air velocity and temperature across the inlet were uniform except for some reduction in velocity within 2 in. of either side[3], the air input to the model and the output of air and heat under the curtain could be obtained from the velocity and temperature distribution along the vertical centre of the inlet.

2.2. Experiments and results

Two series of experiments were carried out; in the first the shapes of burner and vent were varied; in the second the size and position of the curtain and the size of the vent were varied.

2.2.1. Shape of burner and vent

Three types of burner and three shapes of vent were used in these experiments. The burners (linear, circular and double line) are shown in figs. 2A, 2B and 2C respectively. The vents were rectangular having different proportions but the same area of 24 in^2. Details of these experiments are given in Table 1, which also gives the air temperature near the ceiling and the rates of air input and discharge under the edge of the curtain, which were obtained from velocity measurements, as explained above.

TABLE 1

Experiments on effect of shape of vent and burner
(First series)

Vent dimensions in. x in.	Vent position H: over heater I: near inlet	Heater	Curtain depth in.	*Rate of air input ft^3/s	*Rate of discharge of air under edge of curtain ft^3/s	**Rate of discharge of air through vent (by difference) ft^3/s	*Measured temperature near ceiling °F
4 x 6†	H	Line	8	0.42	0.05	0.37	288
		Circular	8	0.41	0.10	0.31	270
12 x 2†	H	Line	8	0.40	0.10	0.30	243
		Circular	8	0.42	0.15	0.27	243
22.5x1.1†	H	Line	8	0.39	0.13	0.26	288
		Circular	8	0.43	0.16	0.27	275
4 x 6‡	H	Double line	12	0.38	0.05	0.33	221
	I	" "	12	0.38	0.05	0.33	220
	H	" "	8	0.59	0.32	0.27	164
	I	" "	8	0.64	0.35	0.29	162

*Obtained from measurements of air velocities.

**Volume measured at ambient temperature.

†Thermocouples arranged as in fig. 1B.

‡Thermocouples arranged as in fig. 1A.

2.2.2. Size and position of vent and depth of curtain

The factors varied in this second series of experiments were the position of the vent, the vent area and the depth of the curtain. Throughout, the vent was approximately square and the circular heater was used. A summary of results is given in Table 2, (page 4).

3. Discussion of results

3.1. Effect of position of vent

The rate of discharge of hot air through the vent (Table 2) was generally greater when the vent was over the heater than when it was near the inlet, although the difference was only important with the 1 in. curtain. In that case it can be explained by the hot gas having a velocity sufficient to cause a tendency to overshoot the vent when this was near the inlet (fig. 3) and to pass under the curtain. This resulted in a correspondingly high rate of discharge under the curtain.

The position of the vent had no significant effect on the temperature near the ceiling.

3.2. Distribution of velocity beneath the curtain

In all the above experiments the rates of air flow were calculated from velocity measurements; a typical distribution of velocity beneath the curtain is shown in fig. 4. The velocity near the floor of the model was 0.5 ft/s with the linear and circular burners and 0.65 ft/s with the double line burner.

Examination of the air flow pattern in the inlet using a smoke tracer showed that in those experiments where there was a high rate of discharge of hot air beneath the curtain a vortex existed between the inflowing and outflowing air streams (fig. 5). This sometimes led to an overestimate of the rate of flow of air into the model as the non-directional anemometer measured the speed of the air in the vortex instead of the mean horizontal velocity.

3.3. Check of experimental measurements

The accuracy of the experimental measurements of air flow and temperature may be estimated by comparing values of the heat passing through the vent calculated in two different ways.

(a) From the net heat input to the model (Q_i) less the heat discharged under the edge of the curtain (Q_s). Q_s is obtained from measurements of air temperature and velocity beneath the curtain.

$$Q_v = Q_i - Q_s \qquad \text{.....(1)}$$

(b) From the temperature and the mass of gas vented, obtained by subtracting the rate of discharge of air under the curtain from the rate of input of air (Tables 1 and 2).

$$Q'_v = \Theta_H C_p (M_i - M_s) \qquad \text{.....(2)}$$

In fig. 6, Q'_v is compared with Q_v. The scatter is rather large, extending from about -25 per cent to +50 per cent.

The rate of flow of heat through the vent could not be obtained from the temperature and velocity of the air flow through the vent because the anemometer calibration was uncertain at the high air temperature existing there. However, the above comparison shows that the vent heat flow can be obtained from measurements of air velocity and temperature beneath the curtain without systematic error except that some very high values of Q'_v were obtained. These are attributed to the difficulties in measuring the air input due to the vortex described in the previous section. Because the first method involves fewer measured quantities in the air streams, it has been assumed that it is more reliable than the second method.

TABLE 2

Results of experiments on size and position of vent and size of curtain
(Second series)

Curtain depth in.	Vent area in^2	Vent position H:over heater I:near inlet	*Rate of air input ft^3/s	*Rate of discharge of air under curtain ft^3/s	†Rate of discharge of air through vent (by difference) ft^3/s	Temperature near ceiling °F
12	16	H	0.29	0.01	0.28	340
		I	0.26	0.03	0.23	354
	24	H	0.36	0	0.36	286
		I	0.29	0.01	0.28	283
	40	H	0.40	0.03	0.37	243
		I	0.35	0	0.35	248
8	16	H	0.41	0.15	0.26	299
		I	0.42	0.22	0.20	308
	24	H	0.49	0.13	0.36	279
		I	0.42	0.05	0.37	262
	40	H	0.46	0.03	0.43	232
		I	0.48	0.07	0.41	241
1	16	H	0.85	0.51	0.34	183
		I	0.67	0.53	0.14	183
	24	H	0.75	0.46	0.29	191
		I	0.93	0.74	0.19	180
	40	H	0.75	0.34	0.41	165
		I	0.80	0.55	0.25	176

*Obtained from measurements of air velocity.

†Volume measured at ambient temperature.

3.4. Distribution of temperature in the model

A typical vertical temperature distribution as recorded by thermocouples 1-12 (fig. 1b) is shown in fig. 7. There is a layer of hot air beneath the ceiling, a layer of cool air near the floor and a central layer where the hot and cold layers are mixing. The variation in temperature over any horizontal plane in the model was found to be small compared with the vertical variation in temperature.

3.5. Effect of shape and position of vent

Both the shape and position of the vent had only a slight effect on the temperature within the enclosure and the heat vented from it; there tended to be slightly more discharge beneath the curtain when the vent was near it. These results are very similar to those obtained in other experiments[1, 5].

4. Calculations of air flow and temperature

The foregoing experiments have determined the heat and air flow through the vent and under the curtain and the temperatures near the roof for various configurations of vent and curtain in a small scale model. In this section a simple theory is developed which enables these quantities to be predicted, in certain cases, from the dimensions and geometry of the model and the size of the fire, and it is shown that the experimental results are consistent with this theory.

4.1. Coefficients of discharge

In the following argument the pressure drop due to the loss of velocity head of the inlet flow beneath the curtain is neglected. This is justified since the layer of hot air beneath the ceiling was at least 4 in. thick and its temperature was of the order of 180°F while the pressure drop across the inlet was equivalent to a head of only about 0.2 in. of air at this temperature.

The rates of discharge of hot gas through the vent and under the curtain may be calculated from the vertical distribution of temperature in the model by using Bernoulli's Theorem (Appendix I). It is, however, found that the actual discharge measured experimentally is less than the theoretical by a factor which is known as the coefficient of discharge. This is usually 0.6 - 0.7[6] but may vary with the size and shape of the orifice and the velocity and orientation of the flow.

4.2. Determination of coefficient of discharge through the vent

It is shown in the appendix that

$$\frac{V_v}{C_d} = A_v \sqrt{\frac{2g\, T_H \int_o^H \theta/T \, dy}{T_o}} \qquad \ldots\ldots\ldots\ldots (3)$$

The integral $\int_o^H \theta/T$ may be evaluated graphically by plotting θ/T against y. This was done for several different configurations of vent and curtain (fig. 8), and by inspection of the graphs, it was found that to a first approximation

$$T_H \int_o^H \theta/T \, dy = \theta_H d \qquad \ldots\ldots\ldots\ldots (4)$$

where d was measured to the point of inflection of the temperature distribution curve, i.e. the shaded area in fig. 8 is approximately equal in area to the rectangle. Hence equation (3) simplifies to

$$\frac{V_v}{C_d} = A_v \sqrt{\frac{2g\, d\, \theta_H}{T_o}} \qquad \ldots\ldots\ldots\ldots (5)$$

V_v/C_d as calculated from equation (5) is plotted against the measured rate of discharge of gas through the vent (fig. 9) (obtained from the subtraction of the measured mass spilled under the curtain from the measured mass input (Table 2)). The results for those experiments where the discrepancy between Q_v and Q'_v exceeded 25 per cent are omitted. Lines corresponding to coefficients of discharge of 0.6 and 0.7 have been drawn on this graph. Although there is a large scatter, the experimental results are consistent with the assumption that the coefficient of discharge is about 0.6 and this value is assumed in all subsequent calculations. In applying the theory to full scale buildings and to vents differing greatly in shape from any discussed in this note, other values for the discharge coefficient may be required.

4.3. Determination of coefficient of discharge under the curtain

If the velocity head of the gas in the upper part of the enclosure may be neglected the curtain behaves as an inverted weir (Appendix)

$$\frac{V_s}{C'_d} = w \int_0^{H_c} \left(\sqrt{2g \frac{T_H}{T_8} \int_0^{\theta/T} dy} \right) dy \qquad \ldots\ldots\ldots (6)$$

This equation was evaluated graphically for a few cases from the experimental temperature distributions and it was found that a similar approximation to that given in the previous section could be used, if the bottom of the hot layer extended at least about 2 in. below the bottom of the curtain. Then as a first approximation equation (6) reduces to

$$\frac{Vs}{C'_d} = \frac{2}{3} w d_c^{3/2} \sqrt{\frac{2g \theta_H}{T_o}} \qquad \ldots\ldots\ldots (7)$$

V_s/C'_d was plotted against the measured volume discharged over the edge of the curtain (fig. 10). Again there is a large scatter, but there is no systematic variation about a line corresponding to a value of 0.6 for the discharge coefficient, though two results in particular are of doubtful value.

4.4. Rate of entrainment of air

The air flow through the vent and under the curtain may be calculated from equations (5) and (7) respectively provided that θ_H and d are known. These latter quantities may be calculated by considering the rate at which the hot air layer is replenished by the rising plume of hot gas and entrained air from the burners (fig. 11). The effect of the rate of input of coal gas in these experiments (0.0175 ft^3/s) may be neglected, in comparison with the much greater rate of flow of air into the hot layer.

The mass of air (M) entrained in a distance (H' - d) by hot gases rising from a point source of heat may be obtained from a formula given by Yih[2] which in our notation may be written

$$M = 0.153 \rho_H \left\{ \frac{Q_f g}{\rho_H C_p T_o} \right\}^{\frac{1}{3}} (H'-d)^{5/3} \qquad \ldots\ldots\ldots (8)$$

Since the fire is not a point source a correction may be introduced based on the angle of spread of the plume as suggested by G. I. Taylor[7].

$$H' = H + 1.5 \sqrt{A_f} \qquad \ldots\ldots\ldots (9)$$

The evaluation of A_f, the effective area of the fire, is discussed in the following section.

4.5. Calculation of temperature beneath the ceiling

The temperature beneath the ceiling can be calculated by substituting

$$M = Q / \theta_H C_p \qquad \text{..... (10)}$$

in equation (8)

$$\frac{\theta_H}{(\theta_H + T_o)^{\frac{2}{3}}} = \frac{6.5\, Q_f^{\frac{2}{3}}}{(\rho_o C_p)^{\frac{2}{3}} (g T_o)^{\frac{1}{3}} (H' - d)^{\frac{5}{3}}} \qquad \text{..... (11)}$$

Since the effective area of the fire in these experiments was not certain, values of θ_H calculated from equation (11) were plotted against d for a number of arbitrary values of H' and compared with the experimental points plotted in the same graph (fig. 12). The most satisfactory agreement between theory and experiment was found if H' was taken to be 25 in., which gives $A_f = 21$ in^2 from equation (9).

As the values of both θ_V and θ_H obtained using the circular burner did not differ significantly from those obtained using the linear burner with the same vent and curtain, it follows that the linear burner had approximately the same effective area as the circular one.

The values of d and θ_H obtained experimentally using the double line burner were put into equation (11) and it was found that this burner had an effective area of 100 in^2.

4.6. Calculation of depth of layer of hot gas

The depth of the layer of hot gas beneath the ceiling is obtained by equating the mass of hot air entering the layer to that discharged through the vent and under the curtain (fig. 11).

When there is no discharge under the curtain

$$M = M_v \qquad \text{..... (12)}$$

From equation (5)

$$M_v = C_d \rho_H A_v \sqrt{\frac{2g\, d\, \theta_H}{T_o}} \qquad \text{..... (13)}$$

and from equations (8), (10), (12) and (13)

$$C_d A_v d^{\frac{1}{2}} = 0.043 (H' - d)^{\frac{5}{2}} \qquad \text{..... (14)}$$

The relevant experimental results are compared with equation (14) in fig. 13. Equation (14) will not apply if $d > H_o$ since the rate of discharge of hot air beneath the curtain must then be taken into account.

$$M = M_v + M_s \qquad \text{..... (15)}$$

From equation (7)

$$M_s = \frac{2}{3} C_d' \rho_H w d_o^{\frac{3}{2}} \sqrt{\frac{2g\, \theta_H}{T_o}} \qquad \text{..... (16)}$$

and from equations (8), (10), (13), (15) and (16)

$$C_d A_v d^{\frac{1}{2}} + \frac{2}{3} C'_d w (d - H_o)^{\frac{3}{2}} = 0.043 (H' - d)^{\frac{5}{2}} \quad \ldots\ldots\ldots (17)$$

The relevant experimental results are compared with equation (17) when $d > H_o$ and with equation (14) when $d < H_o$ in fig. 14. The agreement between theory and practice is very satisfactory in view of the approximations made.

If there is no vent open and all the heat is discharged beneath the curtain equation (17) reduces to

$$C'_d w (d - H_o)^{\frac{3}{2}} = 0.065 (H' - d)^{\frac{5}{2}} \quad \ldots\ldots\ldots (18)$$

4.7. Rates of discharge of air

4.7.1. Through vent - no spill under curtain

The theoretical rate of discharge through the vent when there is no spill under the curtain is obtained by putting the values of d and θ_H obtained from equations (14) and (11) in equation (5). The variation in rate of discharge with vent area calculated in this way and corrected for discharge coefficient, is compared with the experimental points in fig. 15.

4.7.2. Under curtain - no vent

The theoretical rate of discharge under the curtain when there is no vent is obtained by putting the values of d and θ_H obtained from equations (18) and (11) in equation (7). The variation in rate of discharge with curtain depth calculated in this way and corrected for discharge coefficient is compared with the experimental points in fig. 16. In both figs 15 and 16, the agreement is satisfactory.

4.8. Rate of discharge of heat through the vent

The theoretical rate of discharge of heat through the vent is obtained by putting the values of d and θ_H obtained from equations (17) and (11) in the equation (19) below which is derived from equation (5)

$$Q_v = C_d A_v \theta_H \rho_H C_p \sqrt{\frac{2g d \theta_H}{T_o}} \quad \ldots\ldots\ldots (19)$$

The variation in the theoretical value of heat discharged with vent area is compared with the experimental points for two curtain depths in fig. 17. Again, the agreement between theory and practice is satisfactory.

4.9. Summary of Section 4

It has been shown in Section 4 that it is possible to calculate a number of quantities associated with the heat and mass flow in the model and, although there is in some cases a wide scatter in the data, the fact that no significant systematic difference between observed and measured quantities has been found shows that the methods of calculating these quantities, based only on the heat and mass balance using elementary buoyancy considerations and plume theory, are satisfactory.

5. Applications of theory

A theory was developed in the previous section and it was found, by experiment to apply to a particular model. This section shows that the theory may be expected to apply to larger scales of the same model and, in some cases, to other shapes of model.

There is nothing in the foregoing theory that restricts it to any particular scale, provided that the scale is large enough for the flow to be turbulent and that external wind conditions do not influence the flow. There is a restriction on the shape of the enclosure because the experiments have been carried out with a flow which is essentially two-dimensional, i.e. the gases flow along the model or in a vertical direction, but there is no radial flow.

This is because the assumption was made in the theory that the temperature is a function of the height above the floor but is otherwise independent of position; i.e. no mixing occurs between the hot and cold layers. Work on two-dimensional flow systems[8] has shown that little mixing would be expected to occur even when each of the layers is turbulent unless the relative velocity is quite high. Consideration will be given to the problem of radial flow in future work.

5.1. Scaling

For geometrically similar enclosures of linear dimension L, the velocity of the exit hot gases due to the buoyancy of the hot layer is of the form

$$v \propto \sqrt{\theta L} \qquad \ldots\ldots\ldots (20)$$

and the heat balance is of the form

$$Q \propto \frac{\theta v L^2}{T} \qquad \ldots\ldots\ldots (21)$$

Examples of equations similar to equation (20) are (1) - (6) and similar to (21) is (19). Other equations can readily be shown to be combinations of these two types.

From equations (20) and (21)

$$\frac{\theta}{T^{\frac{2}{3}}} \propto \frac{Q^{\frac{2}{3}}}{L^{\frac{5}{3}}} \qquad \ldots\ldots\ldots (22)$$

Equation (11) is of this type

$$\frac{v}{T^{\frac{1}{3}}} \propto \frac{Q^{\frac{1}{3}}}{L^{\frac{1}{3}}} \qquad \ldots\ldots\ldots (23)$$

Equation (8) is of this type (since $M \propto v L^2$).

These relations have been confirmed for the present model using different heat inputs[3]*; they can be used to extend the range of equations (8) - (18) when the linear scales are varied.

---

*These scaling laws are derived for an enclosure in which the exit is the major resistance to flow. For more general systems the relations between L, v, θ and Q are the same but their dependance on T will be different and usually less. To avoid this complication it is desirable to keep the temperatures in a model the same as in the prototype which is being modelled.

5.2. Floor area

Equations (1-13) do not contain the term "floor area", so that nominally they may be applied to buildings of any size. However, as the floor area increases, mixing of the hot and cold layers increases and vents may be slightly less effective as their distance from the fire increases[1, 5]. A similar effect must be expected if heat losses by conduction and radiation through the walls and ceilings are of relatively greater importance than in this model. In general, on large buildings one need only consider the ceiling. This problem has yet to be investigated.

5.3. Effect of area of fire

The depth of the hot layer has been calculated from equation (14) as a function of the effective area of the fire, assuming no discharge beneath the curtain and is shown in fig. 18, for various vent areas. As the effective area of the fire increases the depth of the layer of hot air increases, and if discharge beneath the curtain is to be prevented, larger vents are required. With fires of large area the vent area required may become impractically large, and the discharge of hot gas can only be prevented by restricting the air inlets.

5.4. Effect of inlet openings of limited size on temperature and air flow

Under the conditions of the experiments described in this paper, it is possible to neglect the effect of the pressure drop across the inlet, and therefore to regard the neutral pressure plane as coinciding with the bottom of the hot gas layer. In general, however, the neutral plane will be higher than the bottom of the hot gas layer in order to provide a buoyancy head to balance the velocity head across the inlet (fig. 19). Equations to allow for this can be easily derived, but are generally difficult to solve. There is a simple solution when the bottom of the hot air layer is above the bottom of the curtain and there is no spill under the curtain; the mass rate of flow of gas through the model is then; (See Appendix 2).

$$M = C_d A_i \rho_o \sqrt{\frac{2g\, d\theta_H}{T_H \left(1 + \frac{A_i^2}{A_v^2}\frac{T_H}{T_o}\right)}} \qquad \ldots\ldots\ldots (24)$$

Equation (14) then becomes

$$C_d\, d^{\frac{1}{2}} = 0.043 \left\{\frac{1}{A_i^2}\,\frac{T_o}{T_H} + \frac{1}{A_v^2}\right\}^{\frac{1}{2}} (H'-d)^{\frac{5}{2}} \qquad \ldots\ldots\ldots (25)$$

Thus, if the size of the inlet is reduced so that $\frac{T_o}{T_H}\,\frac{1}{A_i^2}$ cannot be neglected in comparison with $\frac{1}{A_v^2}$ the layer of hot air will be increased in thickness and hence from equation (11) its temperature will be higher. A simple solution is also possible when it can be assumed that the model is full of hot gas at θ_H. This case has been treated by Yokoi[9] and Dyakov[10]. There is evidence[11] that this approximation can be used when a fire covers most of the floor area of the model although it did not appear to hold for the experiments reported elsewhere with a large coal gas fire in a model[5]. These experiments therefore require some future consideration and this will be reported later.

6. Conclusions

The experiments have shown that the shape of the vent is not important and that its position within a small curtained area is only of minor importance provided that the hot air does not have a sufficiently high horizontal velocity to cause a tendency to overshoot the vent. These quantitative results confirm the qualitative results obtained by earlier experiments using a smoke tracer, and it can therefore be inferred that a useful guide may be obtained from simple experiments with a smoke tracer.

The layer of hot gas beneath the ceiling can be regarded as uniform in temperature and Bernoulli's theorem, together with the theory of turbulent plumes can be applied to estimate its depth and temperature. This leads to the following formulae for predicting the efficiency of a vent when the pressure drop across the inlet is negligible and the air flow is linear in a horizontal plane.

(a) Depth of layer of hot air (d)

$$0.6\, A_v\, d^{\frac{1}{2}} = 0.043\, (H'-d)^{\frac{5}{2}} \qquad \text{(fig. 13)}$$

when $d < H_c$

$$0.6\, A_v\, d^{\frac{1}{2}} + 0.4\, (d-H_c)^{\frac{3}{2}} = 0.043 (H'-d)^{\frac{5}{2}} \text{ (fig. 14)}$$

when $d > H_c$

(b) Temperature of hot air layer (θ_H)

$$\frac{\theta_H}{(\theta_H + To)^{\frac{2}{3}}} = \frac{6.5\, Q_c^{\frac{2}{3}}}{(\rho_o C_p)^{\frac{2}{3}}\, (gT_o)^{\frac{1}{3}}\, (H'-d)^{\frac{5}{3}}} \qquad \text{(fig. 12)}$$

(c) Rate of discharge of heat through the vent

$$Q_v = 0.6\, \rho_o\, C_p \left(\frac{To}{T_o + \theta_H}\right) \theta_H \sqrt{\frac{2g\, d.\theta_H}{To}}\, A_v \qquad \text{(fig. 17)}$$

When the model is full of hot gas the analysis of Yokoi[9] may be used.

There is satisfactory agreement between measured and calculated data and it is therefore possible to design a venting system provided the heat output of the fire and the various dimensions of the building are known. Consideration will be given to some problems of design in a later paper using the methods given here.

Acknowledgment

The authors would like to thank Mr. R. W. Claridge for his valuable assistance with the experiments and Miss V. McNaughton for undertaking the calculations.

References

1. SIMMS, D. L., HINKLEY, P. L. and BISSETT, A. Roof venting of burning enclosures, Part 1. Joint Fire Research Organization, F. R. Note No. 390/1959.

2. YIH, C. S. Free convection due to a point source of heat. Proc. 1st U.S. Nat. Congr. Appl. Mech, 1952, 941-7.

3. SIMMS, D. L., HINKLEY, P. L. and BISSETT, A. Roof venting of burning enclosures Part II. Joint Fire Research Organization, F.R. Note No. 391/1959.

4. BIGMORE, R. H. A radiation compensated anemometer. Joint Fire Research Organization, F. R. Note No. 297/1957.

5. THOMAS, P. H. and SIMMS, D. L. On the prevention of flame spread beneath ceilings in fully developed fires by roof vents. Joint Fire Research Organization F. R. Note No. 376/1959.

6. LEWITT, E. H. Hydraulics and the mechanics of fluids, London, 1958, (10th Edition), Sir Isaac Pitman and Sons Ltd.

7. TAYLOR, G. I. The dispersal of fog from airfield runways. ed. WALKER, E. G. and FOX, D. A. Ministry of Supply, London, 1946, p.230 et seq.

8. BAKKE, P. Some Interim Notes on Methane Roof Layers. Safety in Mines Research Establishment Research Report No. 164 Feb. 1959.

9. YOKOI, S. A study on dimensions of smoke vent in fire resistive construction. Report of the Building Research Institute, Tokyo, Japan. No. 29, March 1959.

10. DYAKOV, N. M. Influence of area and space layout of building construction in relation to direction of fire spread. Collected information on fire resistant building construction. Central Research Institute for Fire Protection, Moscow, 1958.

11. SIMMS, D. L., HINKLEY, P. L. and THEOBALD, C. R. Roof venting of burning enclosures, Part IV. Joint Fire Research Organization, F. R. Note (in preparation).

Appendix I

Derivation of formulae for rates of flow of air under the curtain and through the vent

1. Discharge of hot air through the vent (equation 3)

The air is regarded as being stationary inside the model. The pressure beneath the ceiling (p_H) differs only slightly from that outside the model (p_o) so that it is possible to neglect the change in density of the air with pressure on passing through the vent. Bernoulli's equation (which is given together with examples of its use in many text books[6]) may then be written in a simplified form.

$$p_o + \rho_H \frac{V_v^2}{2g} = p_H$$

$$\text{i.e. } V_v = \sqrt{\frac{2g\,(p_H - p_o)}{\rho_H}} \qquad \ldots\ldots\ldots (26)$$

To obtain $(p_H - p_o)$ it is assumed that the temperature, and hence the density, of the air in the model is a function of the height above the floor (y) but is otherwise independent of position. Then (referring to fig. 20)

$$p_H - p_o = \int_o^H (\rho - \rho_o)\, dy \qquad \ldots\ldots\ldots (27)$$

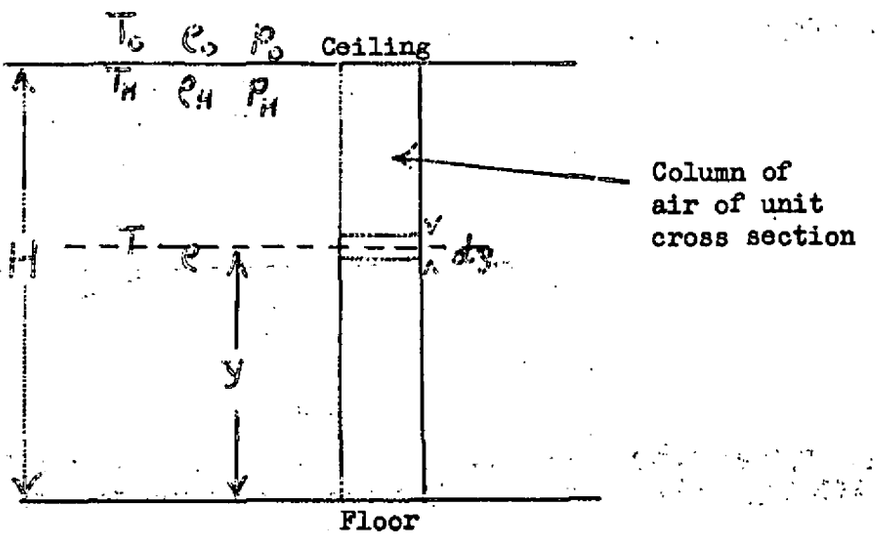

Fig. 20

But $\rho T = p_o T_o = p_H T_H$ ..... (28)

and $T - T_o = \theta$ ..... (29)

Then from equations (26, 27, 28, 29)

$$V_v = \sqrt{\frac{2g\, T_H \int_o^H \theta/T \, dy}{To}} \qquad \ldots\ldots\ldots (30)$$

Now $$V_v = C_d A_v v_v \qquad \ldots\ldots\ldots (31)$$

allowing for the coefficient of discharge as explained in section 4.1.

Equation (3) can be derived from (30) and (31)

$$V_v = C_d A_v \sqrt{\frac{2g\, T_H \int_0^H \theta/T dy}{To}} \qquad \ldots\ldots\ldots (3)$$

2. Discharge of hot air beneath the curtain (equation 6)

Consider a horizontal strip of the opening beneath the curtain at a distance, y, above the floor and having an area W dy (fig. 21).

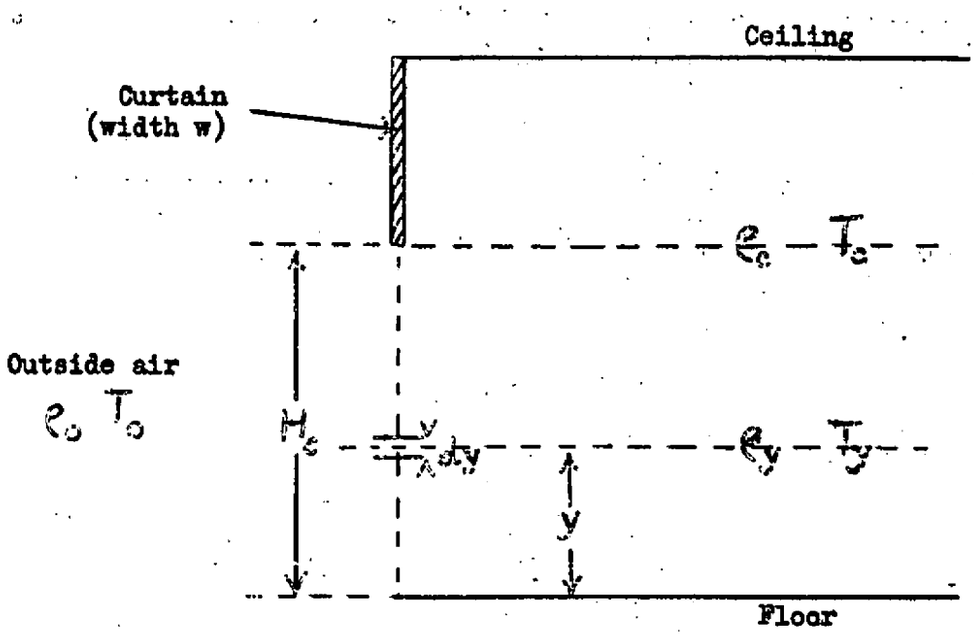

Fig. 21

This may be regarded as a vent at a height, y, above the floor and from equation (3) the discharge (dV) through the strip will be

$$dV = C_d\, w\, dy \sqrt{\frac{2g\, T_y \int_o^y \theta/T \, dy}{To}} \qquad \ldots\ldots\ldots (32)$$

and the discharge through the entire opening (V_s) will be

$$V_s = C_d' \int_o^{H_o} dV = C_d' w \int_o^{H_o} \left(\sqrt{\frac{2\, g\, T_y \int_o^y \theta/T \, dy}{To}} \right) dy$$

This is equation 6.

Appendix II

Derivation of formula for mass flow of air through the model

(equation 24)

A horizontal layer of hot air of temperature T_H, density ρ_H and depth $d < (H - H_o)$ is assumed to exist beneath the ceiling. The rest of the model contains air at T_o and ρ_o (Fig. 22).

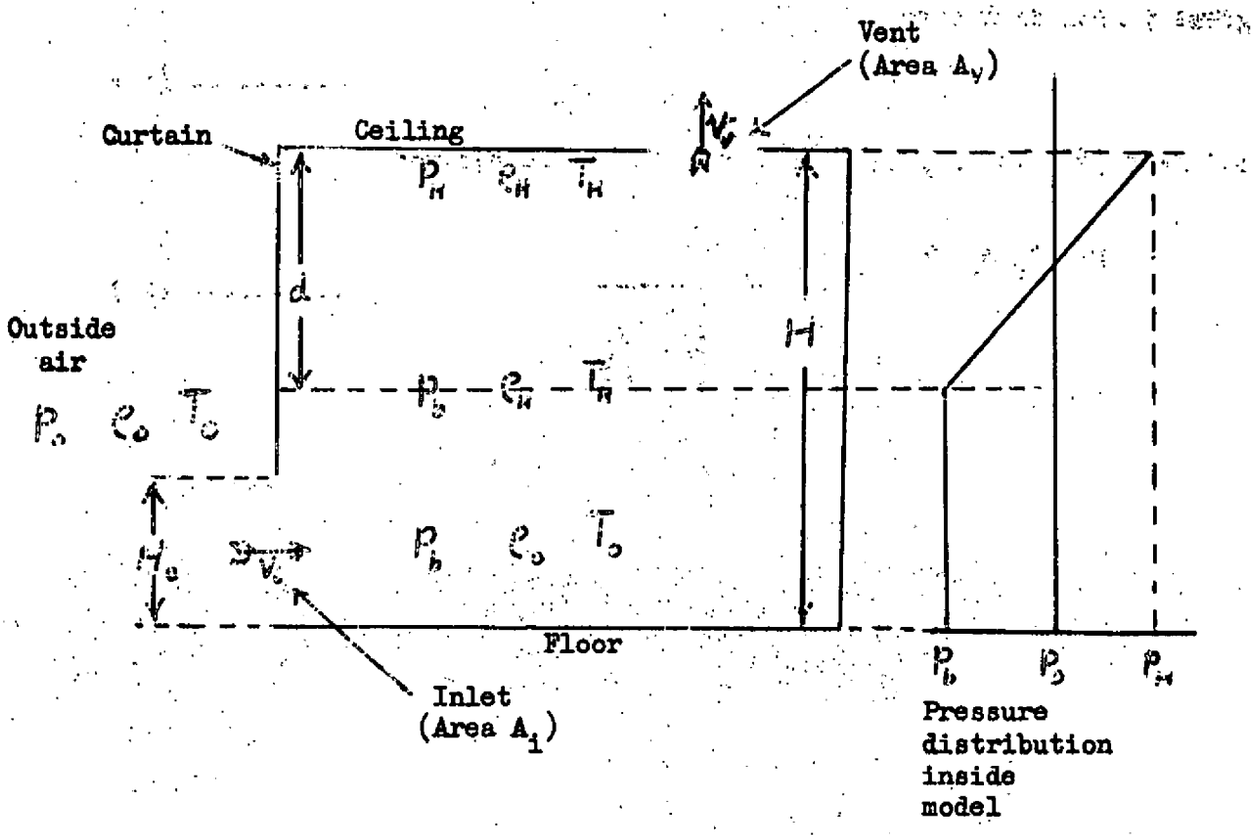

Fig. 22

For the discharge through the vent, Bernoulli's equation may be written

$$p_o + \rho_H \frac{V_v^2}{2g} = p_H \qquad \ldots\ldots\ldots (33)$$

and for air entering through the inlet beneath the curtain

$$p_o = p_b + \rho_o \frac{V_i^2}{2g} \qquad \ldots\ldots\ldots (34)$$

From (33) and (34)

$$p_H - p_b = \rho_H \frac{V_v^2}{2g} + \rho_o \frac{V_i^2}{2g} \qquad \ldots\ldots\ldots (35)$$

But $$p_H - p_b = (\rho_o - \rho_H)d \qquad \ldots\ldots\ldots (36)$$

$$\rho_o T_o = \rho_H T_H \qquad \ldots\ldots\ldots (37)$$

$$\theta = T_H - T_o \qquad \ldots\ldots\ldots (38)$$

Then from equations (35, 36, 37, 38)

$$\theta / T_H \, d = \frac{T_o}{T_H} \frac{V_v^2}{2g} + \frac{V_i^2}{2g} \qquad \ldots\ldots\ldots (39)$$

v_i and v_v can be obtained in terms of the mass flow (M) and the areas of the vent and inlet (A_v and A_i), since

$$M = C_d' A_i \rho_o v_i \quad \ldots\ldots\ldots (40)$$

and $$M = C_d' A_v \rho_H v_v = C_d A_v \rho_o \frac{T_o}{T_H} v_v \text{ (from 37)} \ldots\ldots\ldots (41)$$

Provided that the shapes and areas of the vent and inlet do not differ greatly from each other

$$C_d' \simeq C_d \quad \ldots\ldots\ldots (42)$$

and from (39, 40, 41, 42) equation (24) can be derived

$$M = C_d A_i \rho_o \sqrt{\frac{2g\, d\, \theta_H}{T_H \left(1 + \frac{A_i^2}{A_v^2} \frac{T_H}{T_o}\right)}} \quad \ldots\ldots\ldots (24)$$

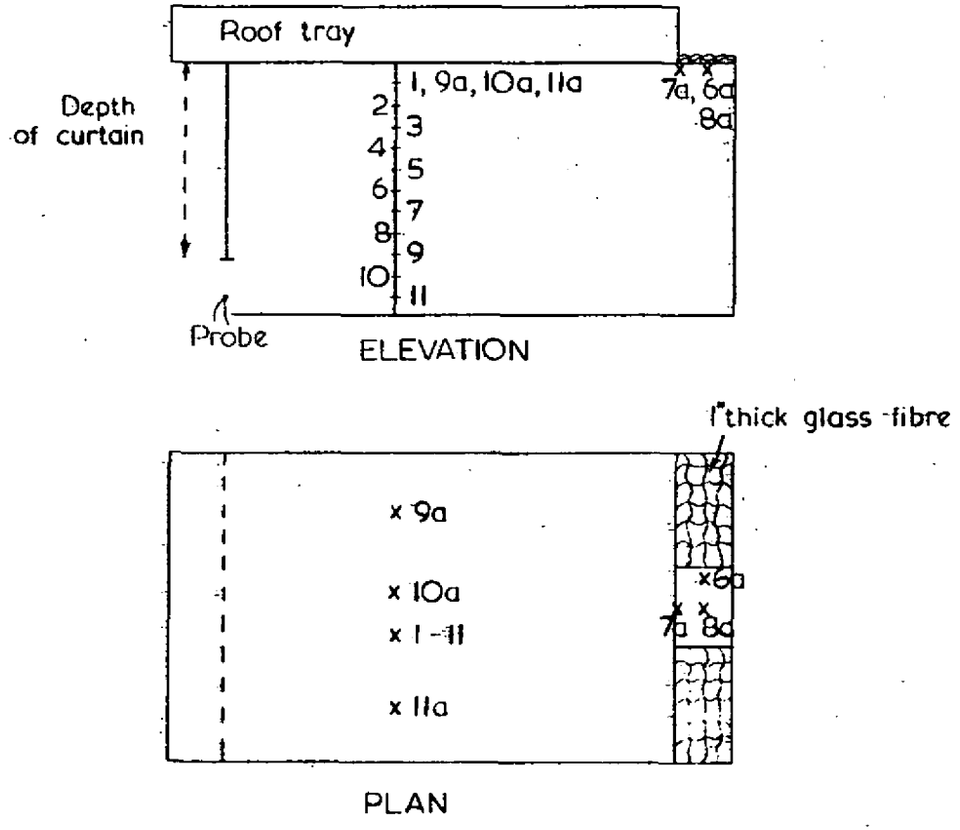

FIG. 1A. DIAGRAM OF MODEL SHOWING POSITION OF THERMOCOUPLES FOR MOST EXPERIMENTS

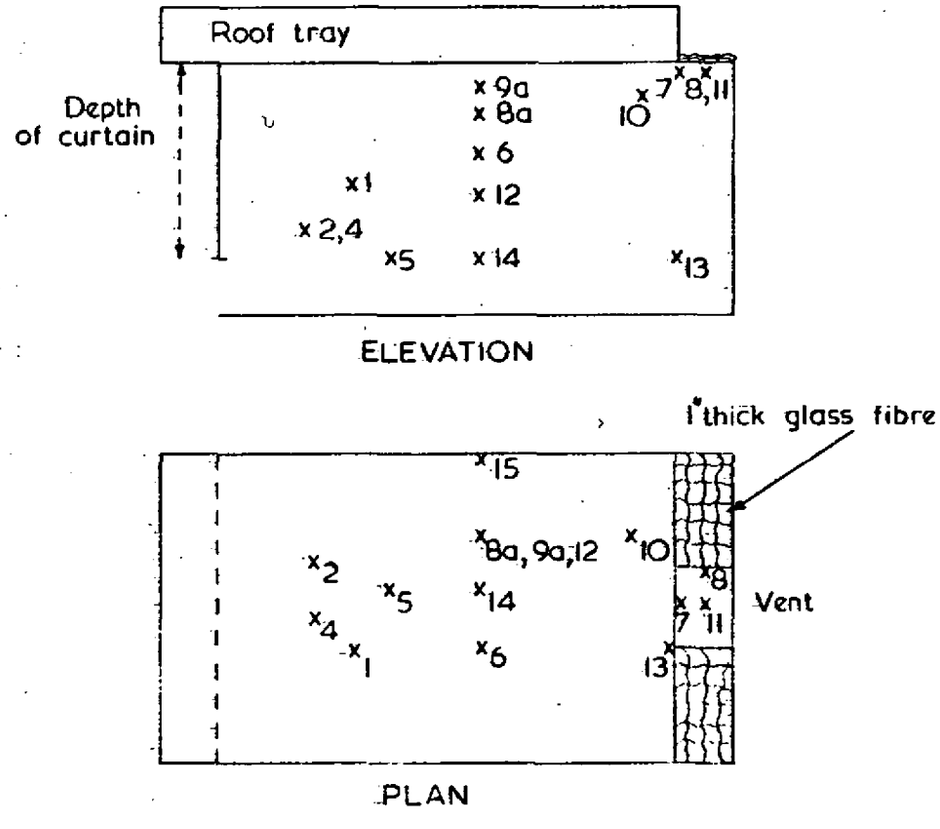

FIG. 1B. DIAGRAM OF MODEL SHOWING POSITION OF THERMOCOUPLES IN SOME EARLY EXPERIMENTS

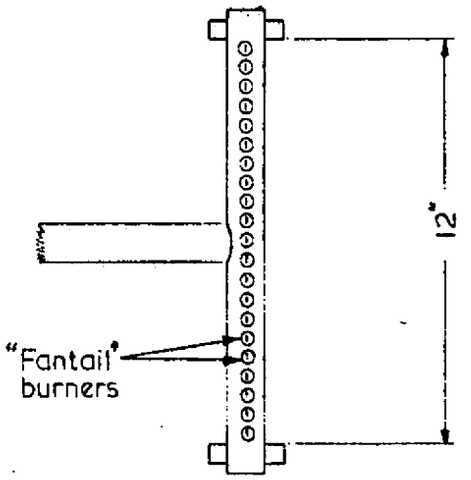

FIG. 2A. LINEAR BURNER

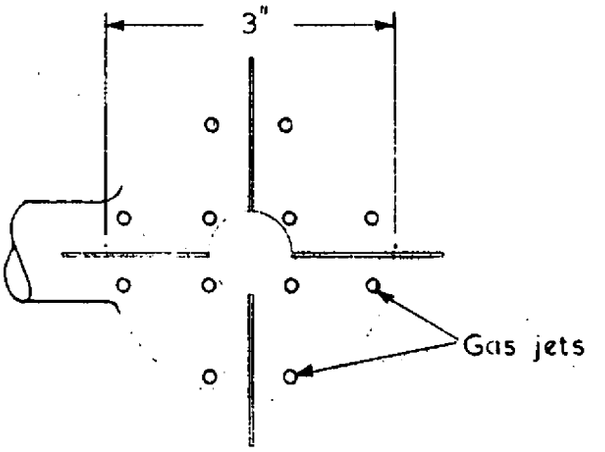

FIG. 2B. CIRCULAR BURNER

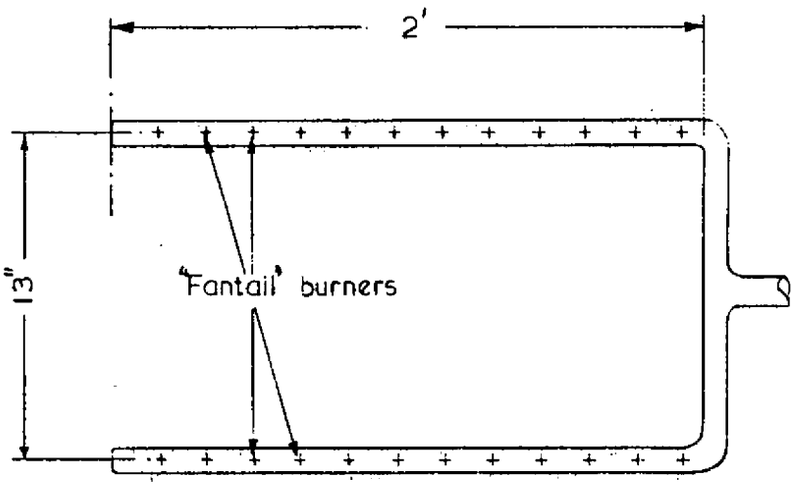

FIG. 2C. DOUBLE LINE BURNER

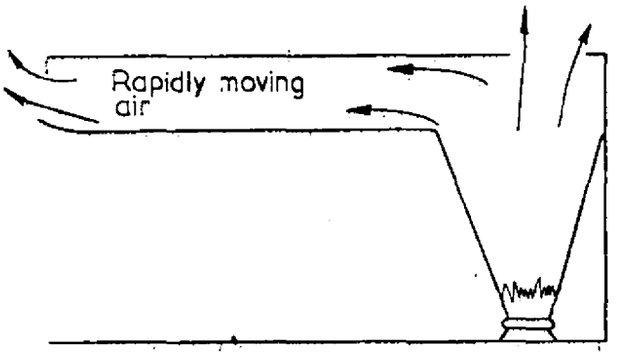

Shallow curtain – vent over heater (No tendancy to "overshoot" vent)

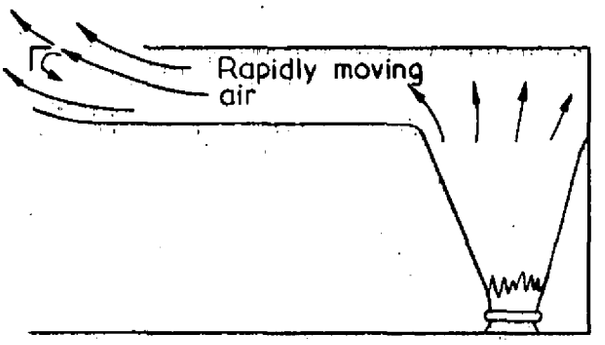

Shallow curtain – vent near inlet
(Considerable tendency to "overshoot" vent)

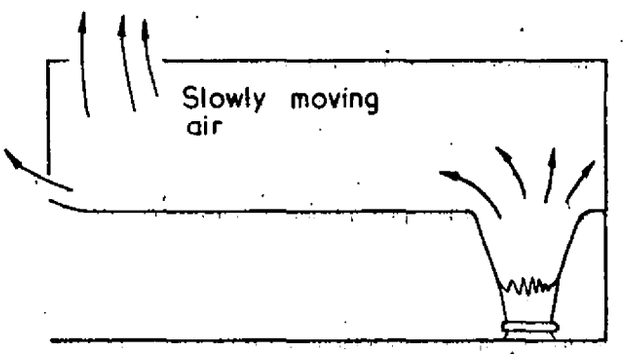

Deep curtain – vent near inlet (No tendency to "overshoot" vent)

FIG. 3. TO ILLUSTRATE TENDENCY OF AIR STREAM TO "OVERSHOOT" THE VENT

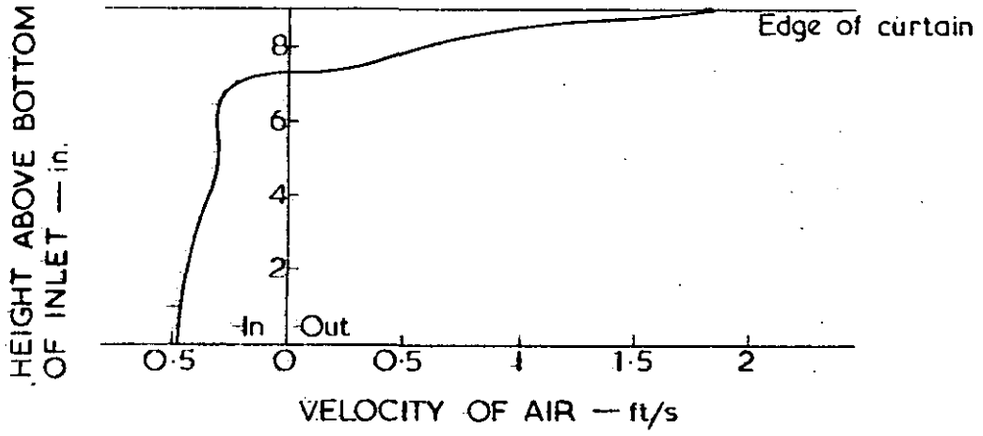

FIG. 4. TYPICAL VELOCITY DISTRIBUTION IN INLET (CIRCULAR BURNER)

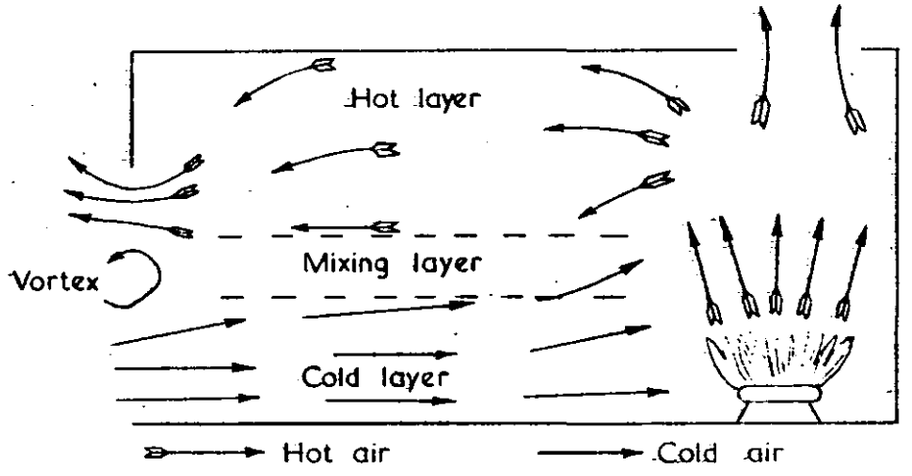

FIG. 5. FLOW INSIDE MODEL WITH GAS HEATING

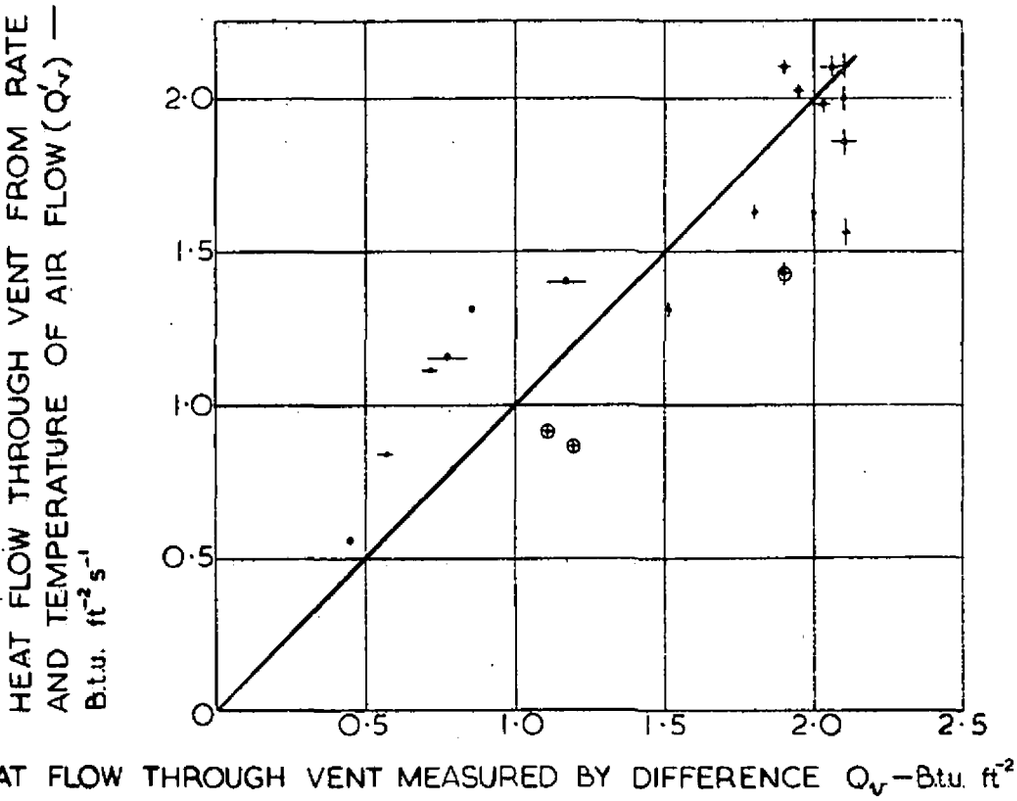

CURTAIN DEPTH — in	VENT AREA — sq in.					
	Circular burners			Distributed burners		
	16	24	40	16	24	40
1	•	–	–			
8	+	+	+		●	
12	+	+	+		●	

Line is for $Q_v = Q'_v$

FIG. 6. COMPARISON OF Q_v WITH Q'_v

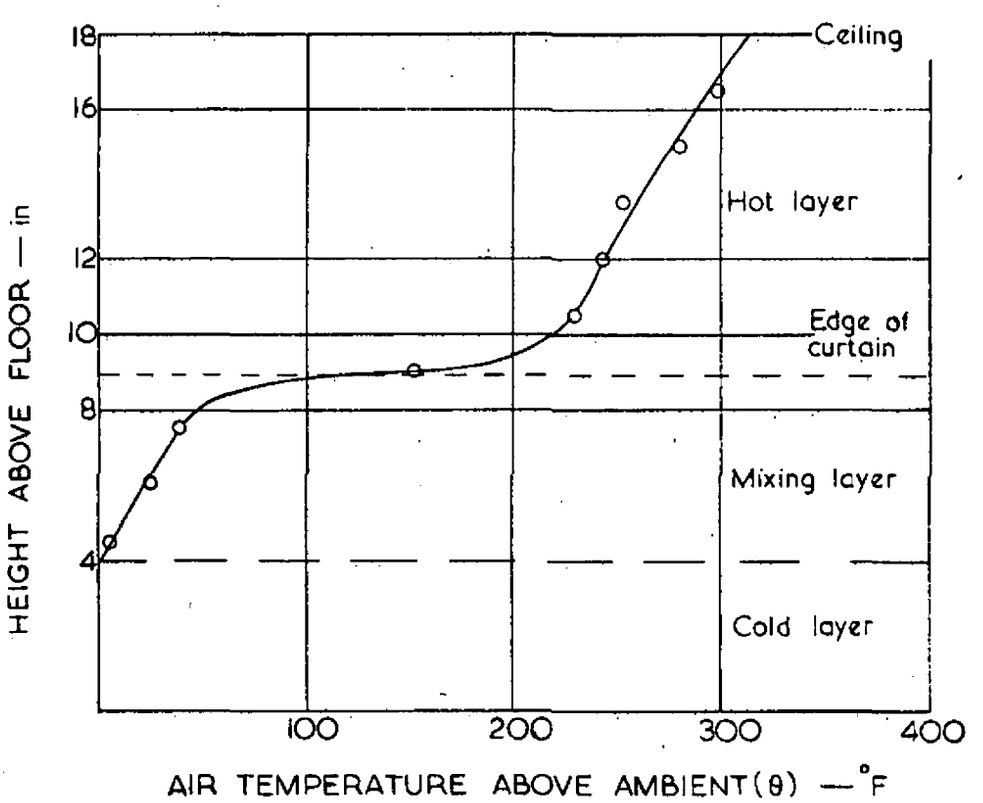

FIG. 7. TYPICAL VERTICAL TEMPERATURE DISTRIBUTION

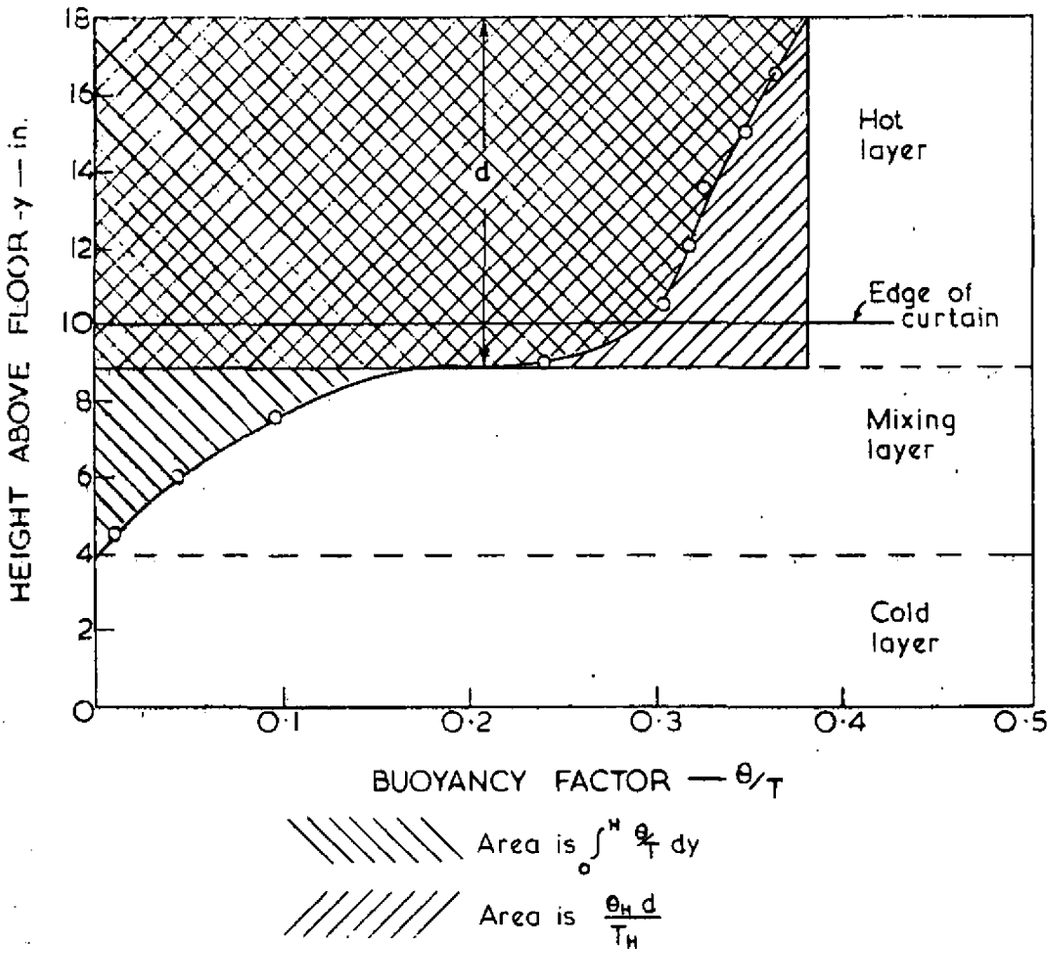

FIG. 8. TYPICAL VERTICAL DISTRIBUTION OF θ/T

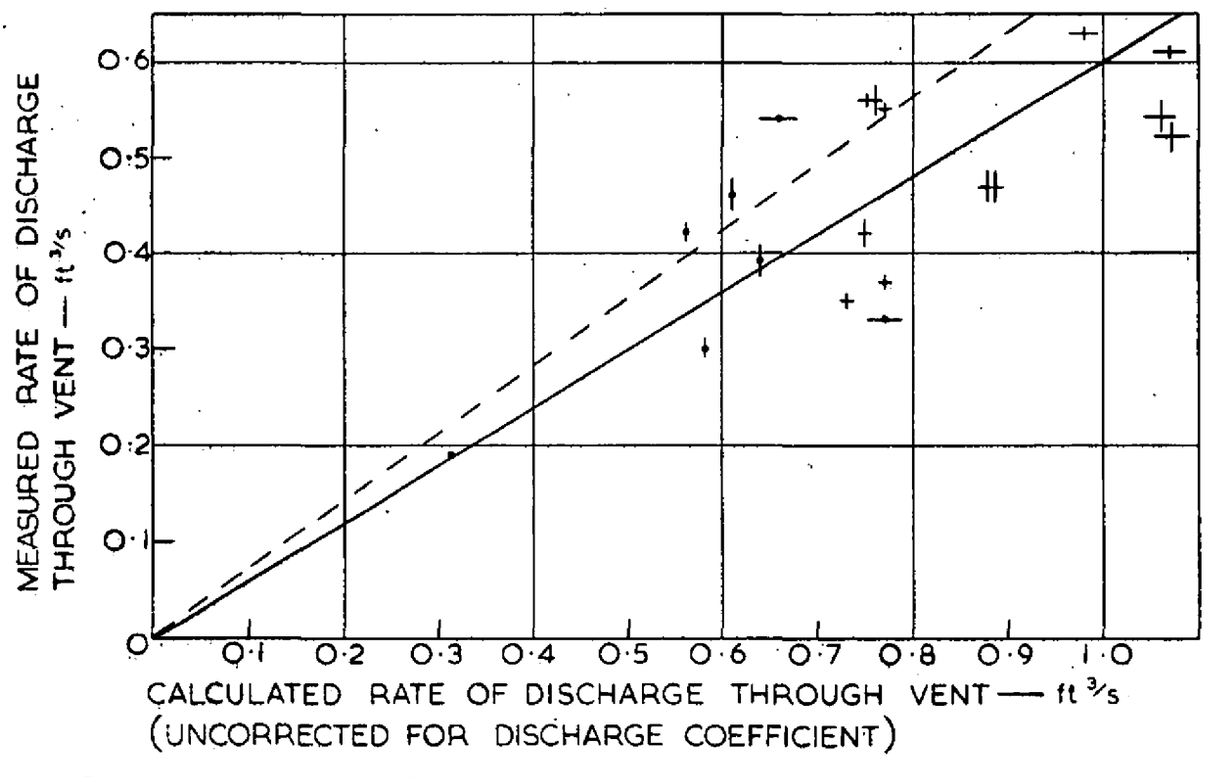

CURTAIN DEPTH – in	VENT AREA – sq in.		
	16	24	40
1	•	•	•
8	+	+	+
12	+	+	+

FIG. 9. COEFFICIENT OF DISCHARGE THROUGH THE VENT

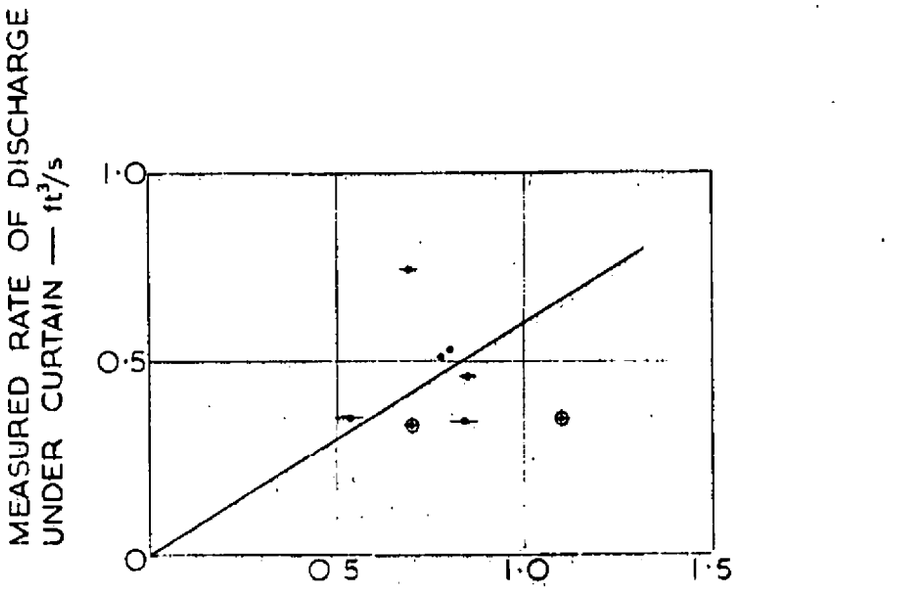

BURNER	CURTAIN DEPTH – in	VENT AREA – sq in.		
		16	24	40
CIRCULAR	1	•	+	+-
DOUBLE LINE	8		⊕	

—— C'd = 0·6

FIG. 10. COEFFICIENT OF DISCHARGE UNDER EDGE OF CURTAIN

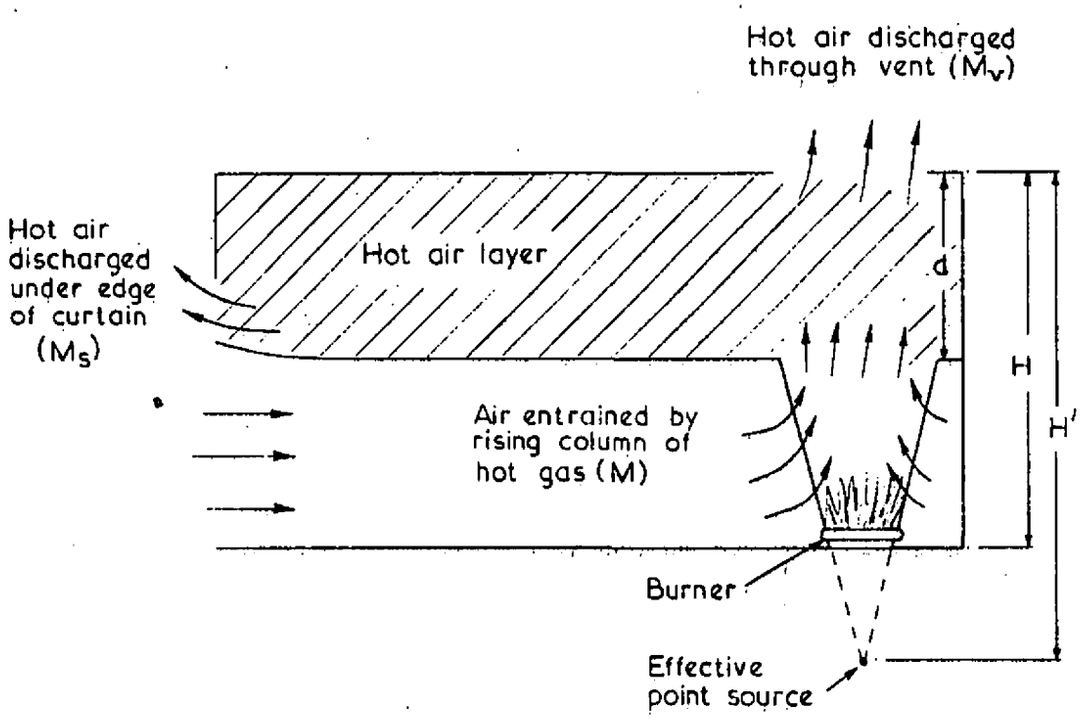

FIG. 11. TO ILLUSTRATE PROCESSES MAINTAINING CONSTANT DEPTH OF HOT AIR UNDER CEILING

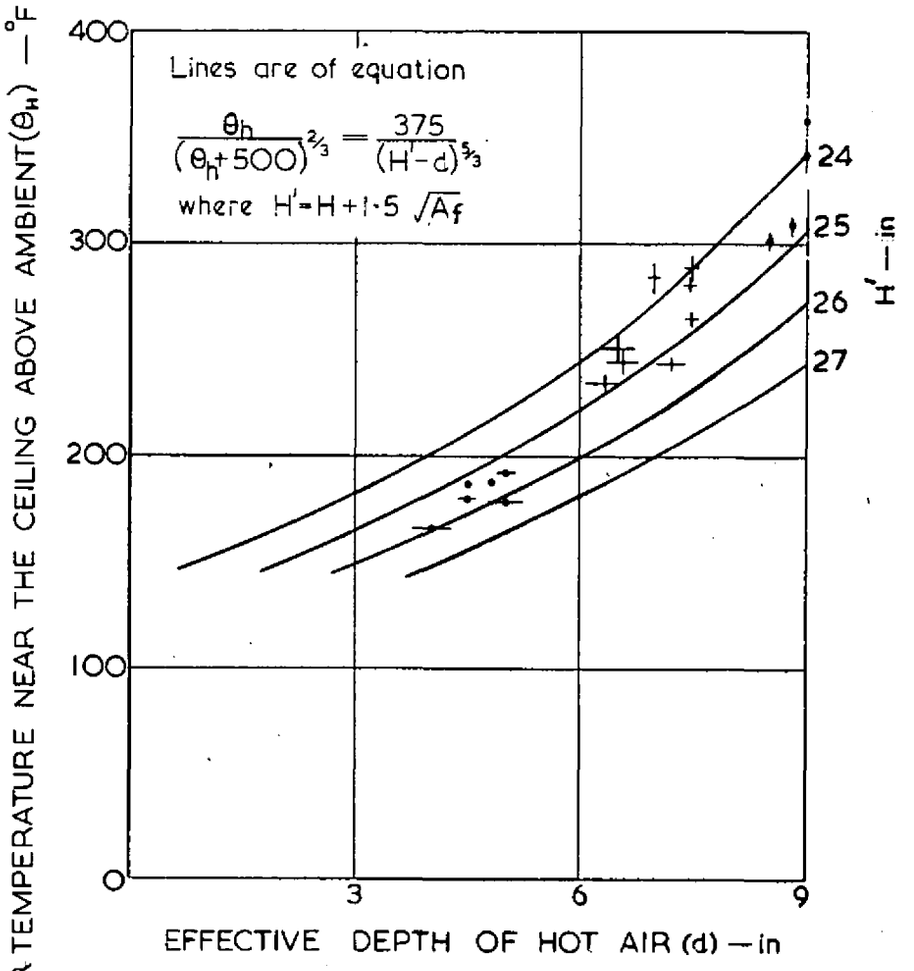

CURTAIN DEPTH — in	VENT AREA — sq in.		
	16	24	40
1	•	•	•
8	+	+	+
12	+	+	+

FIG. 12. TEMPERATURES NEAR THE CEILING

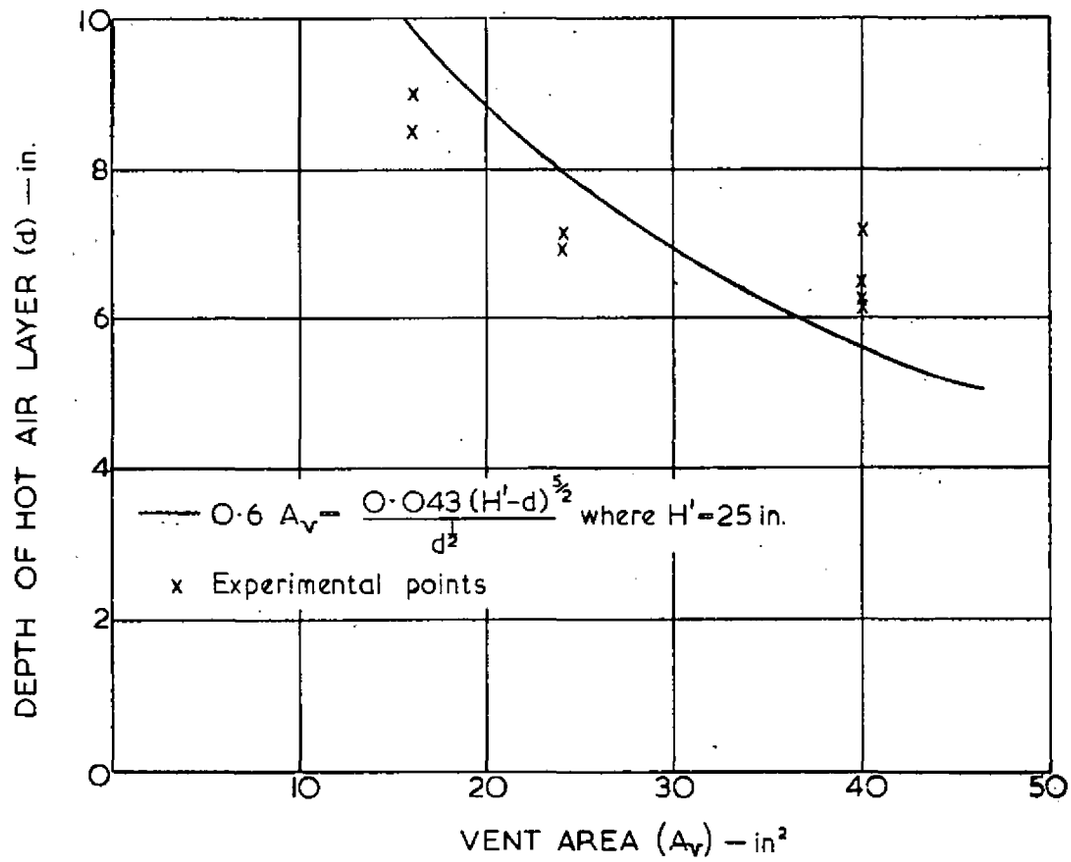

FIG. 13. DEPTH OF HOT AIR LAYER (NO DISCHARGE UNDER CURTAIN)

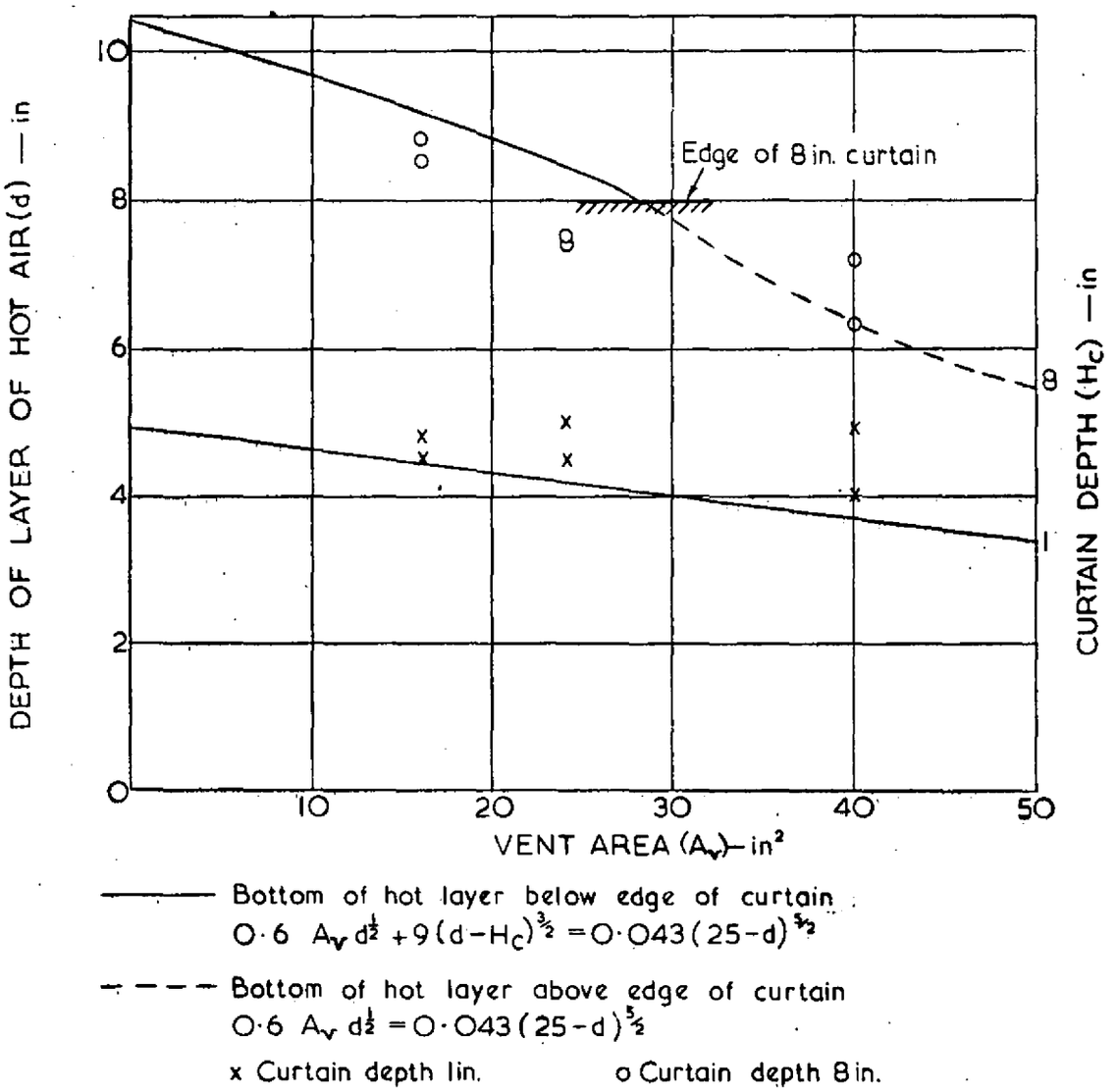

FIG.14. DEPTH OF LAYER OF HOT AIR (GENERAL CASE)

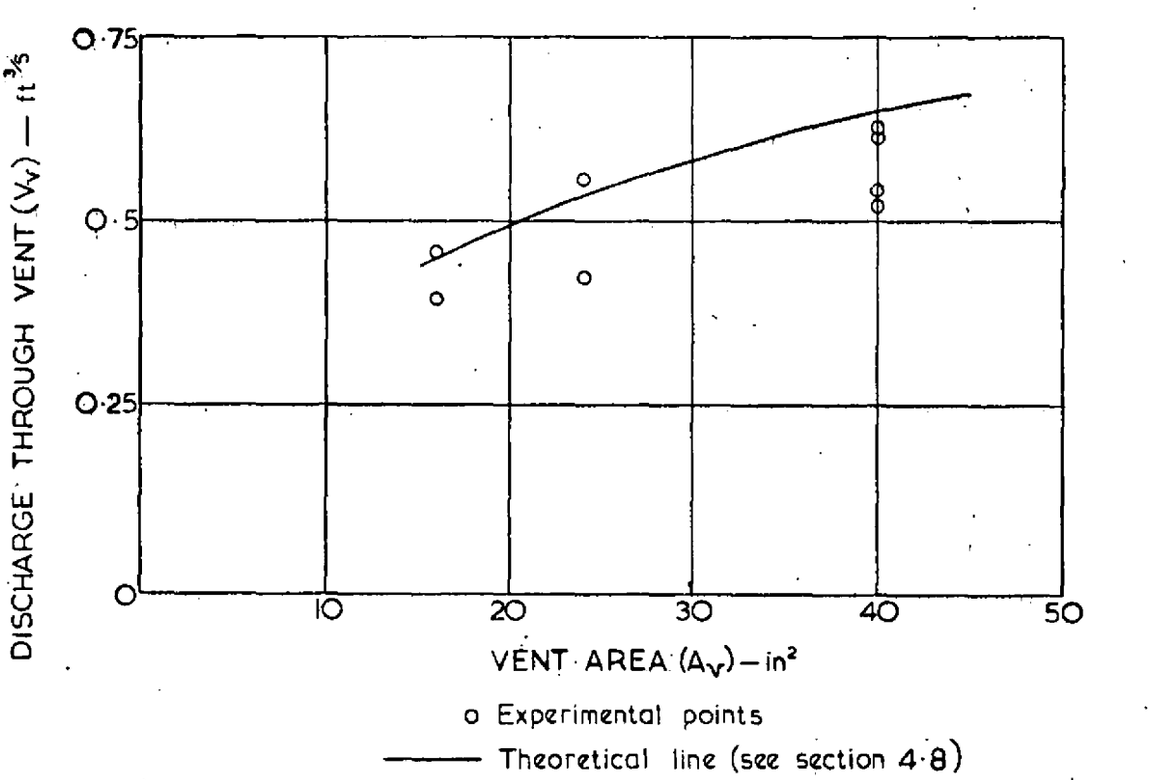

FIG.15. DISCHARGE OF AIR THROUGH VENTS (NO SPILL UNDER CURTAIN)

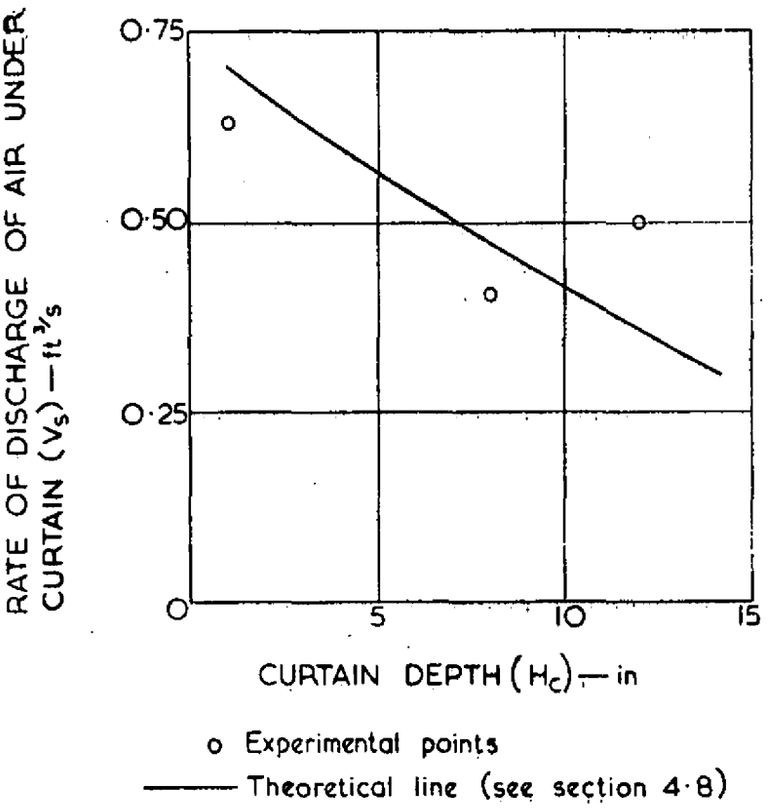

FIG. 16. DISCHARGE OF AIR UNDER EDGE OF CURTAIN (NO VENT)

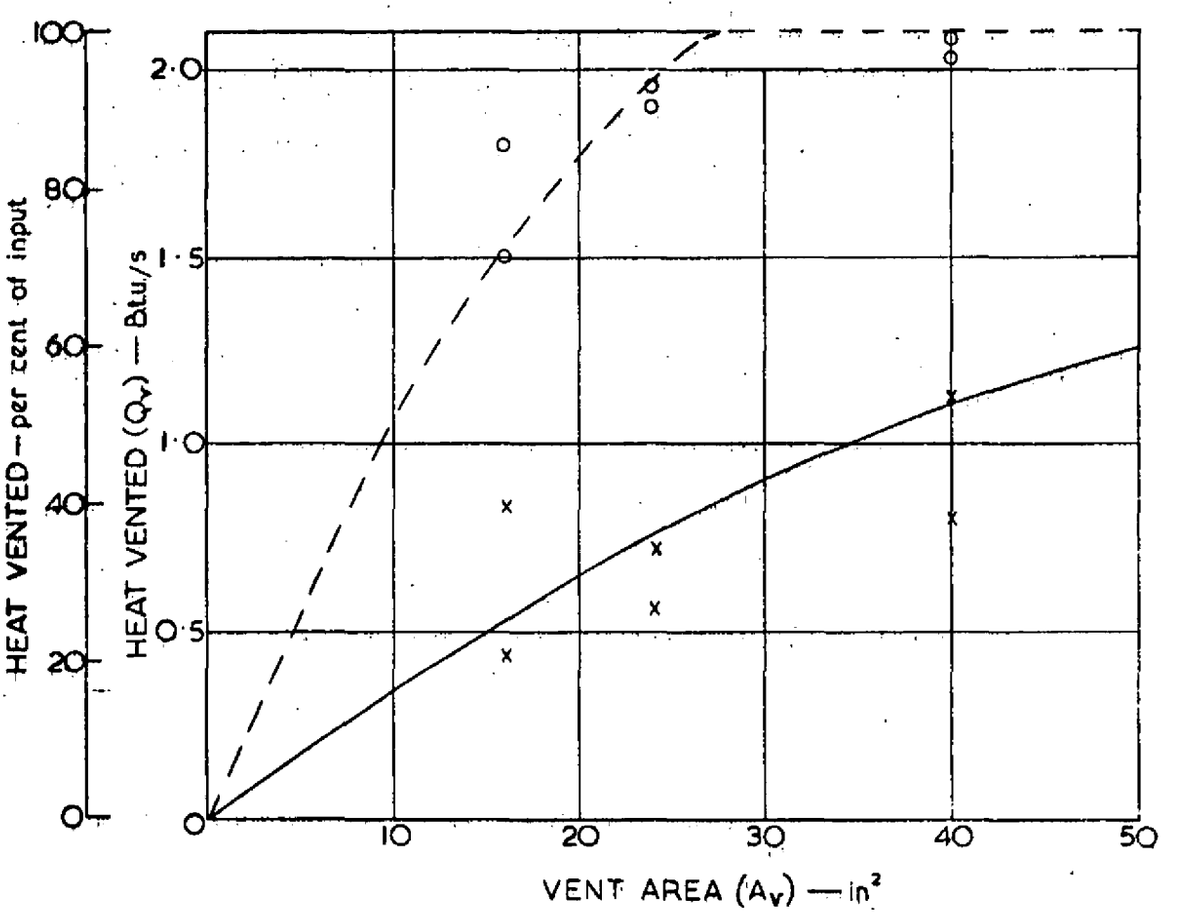

CURTAIN DEPTH – in	EXPERIMENTAL POINTS	THEORETICAL LINES (see section 4·9)
1	x	———
8	o	– – – –

FIG. 17. HEAT VENTED

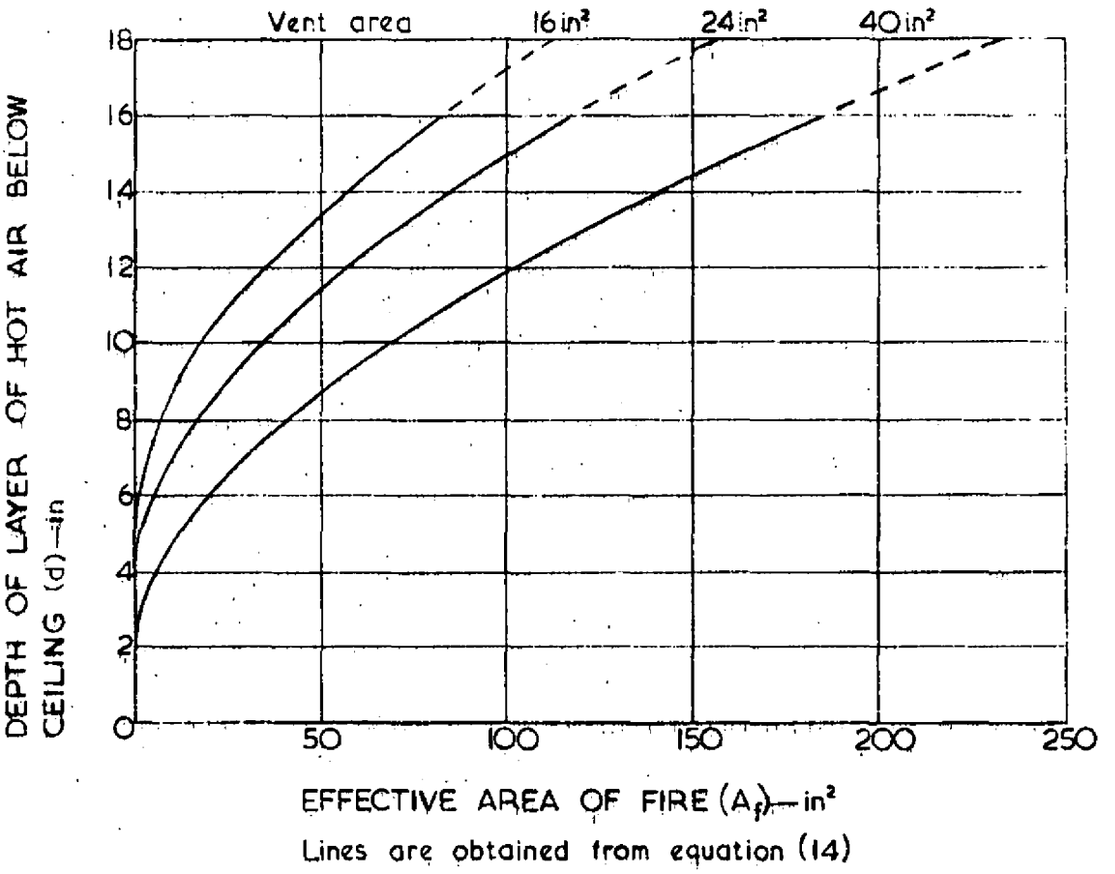

FIG. 18. EFFECT OF FIRE AREA ON DEPTH OF LAYER OF HOT AIR. (NO SPILL UNDER CURTAIN)

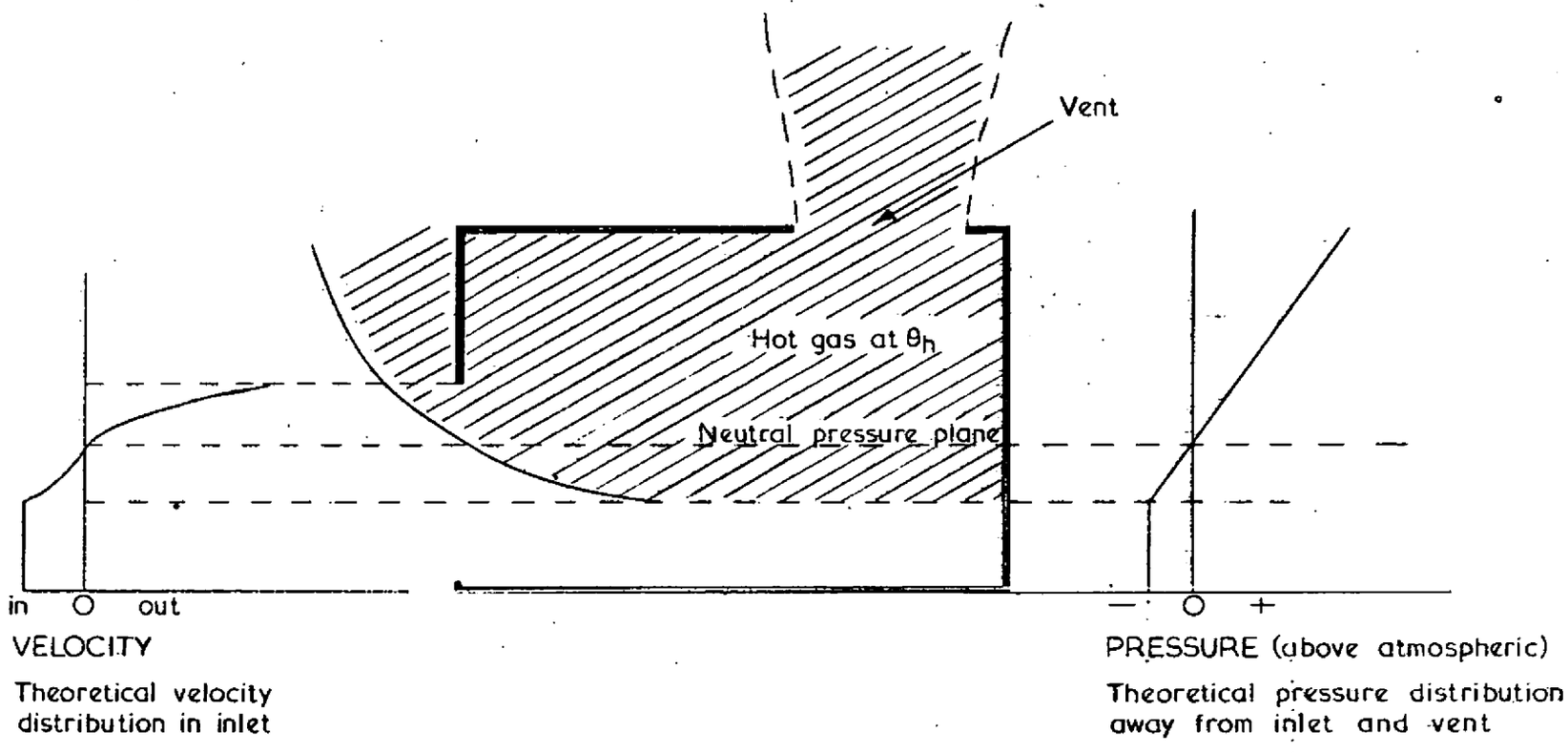

FIG.19. VELOCITY AND PRESSURE DISTRIBUTION IN MODEL